THE OPTICAL PROPERTIES OF NIOBIUM

A. I. GOLOVASHKIN, I. E. LEKSINA, G. P. MOTULEVICH, and A. A. SHUBIN

P. N. Lebedev Physics Institute, Academy of Sciences, U.S.S.R.

The optical constants n and κ (n − iκ is the complex refractive index) of electropolished niobium of an electron-ray melt of 99.9 percent purity are measured in the 0.4 to 10 micron spectral range at helium, nitrogen, and room temperatures. Special x-ray diffraction and optical investigations were carried out which made it possible to prepare the samples without cold hardening and without an oxide film. The main characteristics of the conduction electrons of niobium (the conduction electron concentration N, the mean electron velocity on the Fermi surface v_F, the total area of the Fermi surface S_F, and the effective electron collision frequency ν) and their temperature dependence are derived from data on n and κ in the infrared region of the spectrum. Fourier components of the pseudopotential V_g are derived from measurements in the visible and near infrared regions of the spectrum. The values of V_g are used for determining the conduction electron concentration N; the value is the same as that derived from the measurements in the infrared region of the spectrum. The fact that the two values are equal indicates that the weak-coupling approximation is valid for describing the optical properties of niobium.

THE study of the optical properties of metals makes it possible to obtain the main electron characteristics of the metals: the concentration of conduction electrons N, the total area of the Fermi surface S_F, the mean electron velocity on the Fermi surface v_F, the effective electron collision frequency ν, and the Fourier components of the pseudopotential V_g. This has been carried out for a number of nontransition metals in[1-8]. In this paper we investigate the optical properties of the transition metal niobium and determine its electron characteristics. In order to obtain both the characteristics of the conduction electrons and the Fourier components of the pseudopotential, the optical constants n and κ (n − iκ is the complex refractive index) have been measured in the visible and infrared spectral ranges (0.4—10 μ). Special attention was paid to the quality of the investigated samples.

EXPERIMENTAL PART

1. **Apparatus.** The optical constants were measured at room, nitrogen, and helium temperature by a polarization method on setups described in[2,7,9]. The results of measurements on the different setups agreed with one another.

A UM-2 monochromator was used in the 0.40—0.74 μ range; the radiation detector was an FÉU-38 and the polarizers were polaroids. An IKS-12 monochromator with a glass prism was used in the 0.74—2.6 μ range; the detectors were an FÉU-28 (for the 0.74—1.05 μ range) and an FSA-1 photoresistor (for the 1.00—2.6 μ range), the polarizers were selenium films. A quartz Babinet-Soleil compensator was used in the 0.4—2.6 μ range. In the infrared 2.6—10 μ region we used an IKS-12 with an NaCl prism, a germanium bolometer as the detector, and selenium films as polarizers. The radiation sources were a high-pressure xenon lamp (for the 0.4—1.0 μ region) and a constant-current arc. More

detailed characteristics of the elements of the devices are given in the above mentioned papers.

In the entire spectral range we used fourfold reflection of light from the investigated samples. The spectral width of the slit with which the measurements were made was smaller than or equal to the step of the measurements.

2. **Samples.** Since it was our purpose to obtain the electron characteristics referring to bulk niobium, special attention was paid to the method of preparation of the investigated samples. In view of the small thickness of the skin layer ($\delta \sim 2 \times 10^{-6}$ cm), it is essential that the structure of such a surface coincide with the structure of the bulk metal. Mechanical polishing results in a cold-worked layer whose electron and optical characteristics differ considerably from the characteristics of the bulk metal. We settled on electropolishing, since this method can provide under suitable control a layer of the required quality. The samples in the form of rectangular plates $78 \times 15 \times 5$ mm were prepared from an electron-ray melt of 99.9 percent pure niobium (density 8.57 g/cm^3 and hardness 108 kg/mm^2). After polishing, the samples were annealed at 800°C in a 1×10^{-5} mm Hg vacuum for two hours, in order to relax stresses. The working surfaces were then lapped until flat on lapping plates. This was followed by electrolytic polishing of the samples.

For electropolishing we used an electrolyte[10] containing 850 ml H_2SO_4 and 150 ml HF. The polishing regime was: voltage 20 V, current density ~ 0.8 A/cm^2, and the electrolyte temperature was 40°C. Graphite was used as the cathode. The polishing time amounted to 8—10 min. The time was determined in a special investigation and corresponded to our obtaining a sufficiently flat surface free from cold working. The samples polished in this way had clean mirror surfaces.

This electropolishing regime was chosen as a result of the following additional investigations. We obtained

Table I. Optical constants of niobium

λ, μ	T = 293°K n	T = 293°K κ	T = 78°K n	T = 78°K κ	T = 4,2°K n	T = 4,2°K κ	λ, μ	T = 293°K n	T = 293°K κ	T = 78°K n	T = 78°K κ	T = 4,2°K n	T = 4,2°K κ
0.40	1.50	2.99	1.14	2.93	1.10	3.11	1.50	1.39	8.24	0.66	8.24	0.56	8.24
0.41	—	—	1.17	3.06	1.33	2.94	1.55	—	—	—	—	0.45	8.52
0.42	1.61	2.95	1.51	2.88	1.54	3.00	1.60	1.48	8.96	0.72	8.85	0.41	8.90
0.43	—	—	—	—	1.66	3.01	1.70	1.49	9.61	0.64	9.34	0.41	9.92
0.44	1.91	2.98	1.76	2.97	1.80	3.03	1.75	—	—	—	—	0.28	10.0
0.45	—	—	—	—	1.87	3.08	1.80	1.68	10.3	0.66	10.2	0.28	10.4
0.46	2.00	3.00	1.96	2.99	1.98	3.12	1.85	—	—	—	—	0.22	10.6
0.48	2.02	3.04	2.09	3.04	2.08	3.14	1.90	1.67	11.0	0.54	11.1	0.23	11.0
0.50	2.13	3.07	2.17	3.10	2.24	3.12	1.95	—	—	—	—	0.19	11.4
0.52	2.20	3.08	2.29	3.11	2.28	3.14	2.00	1.75	11.6	0.41	11.4	0.18	11.8
0.53	—	—	—	—	2.31	3.12	2.05	—	—	0.47	11.8	0.28	12.2
0.54	2.23	3.15	2.30	3.12	2.35	3.12	2.10	1.83	12.2	0.66	12.3	0.40	12.6
0.55	—	—	—	—	2.35	3.12	2.15	—	—	0.67	12.5	0.45	12.9
0.56	2.29	3.17	2.36	3.12	2.32	3.09	2.20	2.26	13.1	0.84	12.8	0.63	13.2
0.57	—	—	—	—	2.37	3.12	2.25	—	—	0.78	12.8	0.55	13.5
0.58	2.29	3.23	2.33	3.12	2.38	3.13	2.30	2.33	13.6	0.73	13.4	0.48	14.1
0.59	—	—	—	—	2.35	3.12	2.35	—	—	0.52	13.0	0.40	14.3
0.60	2.27	3.25	2.35	3.16	2.30	3.07	2.40	2.51	14.0	0.50	13.9	0.34	14.4
0.62	2.28	3.25	2.37	3.14	2.30	3.12	2.45	—	—	0.53	14.1	0.33	15.0
0.64	2.27	3.30	2.33	3.15	2.31	3.10	2.50	2.40	14.4	0.70	14.4	0.30	15.3
0.66	2.27	3.36	2.27	3.19	2.28	3.13	2.55	—	—	0.88	14.9	0.45	15.7
0.68	2.23	3.38	2.25	3.16	2.26	3.14	2.60	2.58	15.3	0.99	14.9	0.83	16.1
0.70	2.22	3.41	2.15	3.12	2.17	3.19	2.75	—	—	—	—	0.90	16.6
0.72	2.17	3.44	2.12	3.15	2.14	3.25	2.80	3.17	16.3	1.40	16.2	—	—
0.74	2.13	3.47	2.05	3.25	2.11	3.24	3.00	3.65	17.3	1.63	17.4	1.10	17.3
0.76	2.11	3.62	1.95	3.28	2.02	3.40	3.30	—	—	1.86	17.5	1.26	17.7
0.78	2.06	3.72	1.80	3.48	1.85	3.62	3.50	4.55	19.8	—	—	1.53	18.5
0.80	2.05	3.85	1.79	3.57	1.69	3.69	3.70	—	—	2.36	18.6	—	—
0.82	2.01	3.90	1.72	3.64	1.64	3.72	4.00	5.62	22.2	—	—	—	—
0.84	2.00	4.03	1.67	3.74	1.60	3.78	4.22	5.79	23.4	2.60	24.4	1.82	24.7
0.85	1.92	4.06	1.65	3.88	1.63	4.06	4.50	6.72	25.1	—	—	—	—
0.86	—	—	—	—	1.51	4.05	4.70	7.46	26.8	2.81	28.2	2.04	28.4
0.88	1.86	4.16	—	—	1.49	4.10	5.00	8.06	27.7	—	—	—	—
0.90	1.83	4.32	1.58	4.13	1.47	4.19	5.50	9.20	29.6	—	—	—	—
0.92	1.80	4.41	—	—	1.39	4.33	5.90	—	—	—	—	2.70	35.9
0.94	—	—	—	—	1.31	4.40	6.00	10.4	31.0	3.79	35.7	—	—
0.95	1.71	4.62	1.39	4.40	1.33	4.47	6.20	10.7	32.7	—	—	—	—
0.98	1.71	4.80	—	—	1.24	4.67	6.50	11.5	33.9	—	—	—	—
1.00	1.66	4.94	1.28	4.73	1.23	4.82	6.60	—	—	4.75	38.2	—	—
1.05	1.59	5.37	1.11	5.01	1.10	5.15	6.70	—	—	—	—	3.40	38.4
1.10	1.52	5.66	1.03	5.45	1.01	5.60	6.80	12.5	34.8	—	—	—	—
1.15	—	—	—	—	0.97	6.15	7.00	13.1	36.2	—	—	—	—
1.20	1.43	6.31	0.86	6.12	0.82	6.28	7.50	15.1	37.4	—	—	—	—
1.30	1.38	7.04	0.80	6.89	0.78	7.03	8.00	16.3	38.8	—	—	—	—
1.40	1.35	7.64	0.78	7.40	0.75	7.51	8.20	—	—	6.15	50.5	4.04	51.0
1.45	—	—	—	—	0.62	8.00	9.00	19.2	41.0	—	—	—	—
							9.20	—	—	6.45	58.5	4.99	58.8
							10.00	22.4	44.3	—	—	—	—

x-ray photographs (by the back-reflection method) of one mechanically polished and of three electropolished samples with layers of 15, 50, and 80 μ removed. In the case of the mechanically polished sample it was difficult to discern lines on the x-ray pattern. In the case of the sample with a 15-μ removed layer which had already, by the way, a mirror surface the lines are noticeable but diffuse. This attests to a considerable distortion of the lattice in the surface layer of these samples. In the case of the sample with a 50-μ layer removed the lines are sharp. A further increase of the thickness of the removed layer to 80 μ does not change the sharpness of the lines. Thus, in order to obtain a niobium surface without cold working, it is sufficient to remove a layer of 50 μ. The thickness of the layer removed cannot be decreased appreciably since we showed in[11] that for Nb-Ti alloys which are harder than niobium the thickness of the cold-worked layer is no less than 40 μ. It should be noted that in the case of the samples of Nb alloys with Ti[11] we investigated the correlation between the form of the x-ray photographs and the change of the optical constants for different thicknesses of the removed layer. The change in the optical constants of the electropolished samples compared with mechanically polished ones is considerable, and the constants cease to vary only for such thicknesses of the removed layer which correspond to the appearance of sharp lines on the x-ray pattern. The polishing time

was thus determined by the condition that a 50-μ layer be removed.

In order to clarify the effect of an oxide layer on the optical constants of niobium, we carried out the following measurements. First, we investigated whether an oxide layer does not appear during electropolishing. To this end we measured immediately after the electropolishing the optical constants at a single wavelength for various angles of incidence of the light. The optical constants did not depend on the angle of incidence. This indicates that either there is no oxide layer or it is so thin that it does not affect the measurements of the optical constants. Secondly, we investigated the problem of the appearance of an oxide layer with time. To do this, we measured the optical constants directly after electropolishing, after 24 hours, after a few days, after a week, after two weeks, and after a month. It turned out that in the infrared spectral range the optical constant remained practically unchanged. Even after a month the charges were within experimental error. In the visible region of the spectrum the change of n and κ was noticeable after a week; after two weeks the optical constants changed by about 10 percent. Each series of measurements began directly after electropolishing and took no longer than 3—4 days. It can therefore be assumed that the oxide layer had no effect on the results of the measurements.

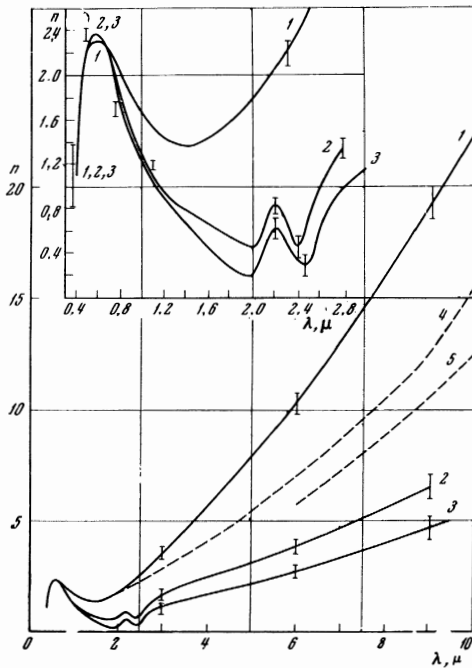The measurements of the optical constants were first

FIG. 1. Refractive index of niobium: 1 – T = 293°K, 2 – T = 78°K and 3 – T = 4.2°K – present work; 4 – according to [12], 5 – according to [13,14].

FIG. 2. Adsorption index of niobium. For notation see the caption of Fig. 1.

carried out at room temperature, and then using the same samples at nitrogen and helium temperatures. After these the measurements were repeated for control purposes at room temperature. The results of the measurements of n and κ carried out at room temperature at the beginning and at the end of each series agreed with one another.

It can thus be assumed that the results of this work refer to bulk metal with an undistorted lattice.

RESULTS OF THE MEASUREMENTS

Several series of measurements were made at each temperature (293, 78, and 4.2°K). The obtained values of n and κ averaged over all series are given in Table I. The dependence of the surface impedance on the angle of incidence was taken into account in accordance with the formulas of [2].

Figures 1 and 2 show the experimental $n(\lambda)$ and $\kappa(\lambda)$ curves for the three temperatures. The errors in the determination of the optical constants in the individual regions of λ are also indicated. They were determined from the spread of the values in the various series of experiments. Within a single series of measurements the errors were smaller than those indicated.

From Table I and Figs. 1 and 2 one can draw the following conclusions:

1. In the long-wave region $(3-10\,\mu)$ both n and κ increase monotonically with the wavelength λ. n decreases with decreasing temperature, the change from room temperature to nitrogen temperature being considerably greater than from nitrogen to helium temperature. It should be noted that the decrease of n on going from nitrogen to helium temperature is rather large. This attests to the good quality of the samples.
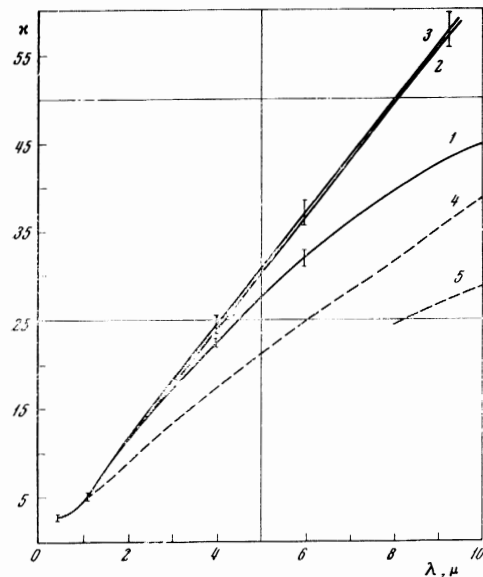
The absorption index κ increases with decreasing temperature, its increase on going from room to nitrogen temperature being considerably greater than on going from nitrogen to helium temperature. The behavior of the functions $n(\lambda, T)$ and $\kappa(\lambda, T)$ is characteristic for conduction electrons.

2. In the short-wave region $(0.4-3.0\,\mu)$ we observed maxima on the $n(\lambda)$ curve and a kink in the $\kappa(\lambda)$ curve; these are connected with interband transitions. The sharp maximum of $n(\lambda)$ in the $0.5-0.7\,\mu$ region appears at all temperatures. At nitrogen and helium temperatures its magnitude and width are almost equal. At room temperature it is somewhat lower and broader. The second maximum of $n(\lambda)$ in the $2.0-2.5\,\mu$ range is considerably weaker and is only observed at 4.2 and 78° K.

It should also be noted that at nitrogen and helium temperatures the effect of interband transitions on the optical properties is also appreciable in the $2.5-3.0\,\mu$ range.

In Figs. 1 and 2 we present the optical constants of niobium at room temperature obtained in [12-14]. Mechanical polishing without control of the structure of the surface layer of the samples was employed in these papers. It is seen from Figs. 1 and 2 that the values of n and κ of mechanically polished samples differ considerably from the optical constants of the undistorted metal. The results of Kirillova and Charikov[12] are appreciably closer to our data, a fact which is apparently related to their use of mechanical polishing in an acid medium. Lenham and Treherne[14] carried out measurements at 95, 90, and 30° K. The temperature dependence of n and κ which they obtained is considerably smaller than in our paper; this also attests to the considerable effect of the cold-hardened layer on the optical constants of niobium obtained in[14].

THE PROCESSING OF THE EXPERIMENTAL DATA

1. **Long-wave region.** Let us first consider the spectral range in which the optical properties are deter-
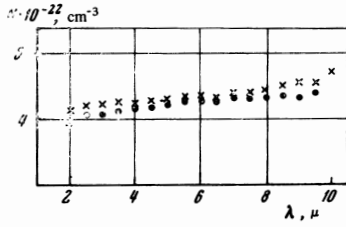
FIG. 3. Concentration of conduction electrons of niobium: $\times$ — T = 293°K, ● — T = 4.2°K.

FIG. 4. Effective collision frequency of conduction electrons of niobium: $\times$ — T = 293°K, ○ — T = 78°K, ● — T = 4.2°K.

mined by the conduction electrons. As will be seen below, there is a weakly anomalous skin effect in niobium at all temperatures. The calculation of the microcharacteristics was therefore carried out in accordance with the following formulas:[5,15]

$$N = \frac{0.1115}{\lambda^2} \cdot 10^{22} \varkappa^2 \frac{(1 + n^2/\varkappa^2)^2}{1 - n^2/\varkappa^2} \frac{1}{1 - \beta_1}, \tag{1}$$

$$\nu = \frac{37.67}{\lambda} \cdot 10^{14} \frac{n/\varkappa}{1 - n^2/\varkappa^2} \frac{1 - \beta_2}{1 - \beta_1}, \tag{2}$$

$$\beta_1 = 0.1251 \cdot 10^{-10} \langle v_F \rangle \varkappa \frac{1 + n^2/\varkappa^2}{1 - n^2/\varkappa^2} \frac{v/\omega - n/\varkappa}{1 + v^2/\omega^2}, \tag{3}$$

$$\beta_2 = 0.06254 \cdot 10^{-10} \langle v_F \rangle \varkappa \frac{1 + n^2/\varkappa^2}{n/\varkappa} \frac{1 + (n/\varkappa)(v/\omega)}{1 + v^2/\omega^2}. \tag{4}$$

Here N (cm^{-3}) is the concentration of conduction electrons, ν (sec^{-1}) is effective collision frequency of the conduction electrons, $\langle v_F \rangle$ is the mean value of the velocity of electrons on the Fermi surface (cm/sec), $\omega = 1.884 \times 10^{15}/\lambda$ is the angular frequency of the light (sec^{-1}), $\lambda(\mu)$ is the wavelength of the light, and β_1 and β_2 are corrections connected with the anomalous nature of the skin effect.

In Eqs. (1)–(4) the mean velocity of the electrons enters only in the correction terms; N and ν are therefore not particularly sensitive to the value of $\langle v_F \rangle$. For calculating $\langle v_F \rangle$ and S_F we used expressions obtained in the weak-coupling approximation[5] (the reasons for such an approximation will be given below):

$$\langle v_F \rangle / v_F^0 = \sqrt{N / N_{val}}, \tag{5}$$

$$S_F / S_F^0 = \sqrt{N / N_{val}}. \tag{6}$$

Here N_{val} is the concentration of valence electrons, and S_F is the total area of the Fermi surface; the superscript zero signifies that the corresponding quantity refers to the conduction electrons at a concentration equal to the valence concentration.

The calculation in accordance with formulas (1)–(5) was carried out by the method of successive approximations on an electronic computer; the number of approximations was determined by the accuracy of the calculation which amounted to about 0.1 percent for all wavelengths and the various temperatures. The number of approximations was 2–3. In the calculation we used the values $N_{val} = 27.8 \times 10^{22}$ cm^{-3}, $v_F^0 = 2.34 \times 10^8$ cm/sec, and $S_F^0 = 5.65 \times 10^{-37}$ g^2-cm^2/sec^2. The results of the calculation of N and ν are shown in Figs. 3 and 4.

The corrections β_1 and β_2 are small compared with unity. Thus $\beta_1 \sim 0.01$ and $\beta_2 \sim 0.05$ for T = 293°K, $\beta_1 \sim 0.002$ and $\beta_2 \sim 0.2$ for T = 78°K, and $\beta_1 \sim 0.001$ and

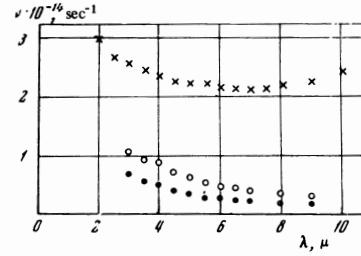$\beta_2 \sim 0.3$ for T = 4.2°K. The skin effect is thus weakly anomalous at all temperatures. It should be noted that the use of the formulas of the normal skin effect at low temperatures leads to appreciable errors since in this case β_2 amounts to about 30 percent and $l/\delta \sim 1$ (l is the mean free path of the electrons and δ is the depth of the skin layer).

For determining the microcharacteristics of the conduction electrons one must use experimental data referring to that region of the spectrum in which one can neglect the influence of the interband transitions. In this region the values of N and ν should not depend on λ. As is seen from Figs. 3 and 4, the 5–10 μ range can be considered to be such a region for niobium. The mean values of the electron characteristics in this region are presented in Table II.

Let us indicate for comparison that for mechanically polished niobium the values of N are considerably lower than for electropolished niobium. Thus, according to the data of[12] N = 2.4×10^{22} cm^{-3}, according to the data of[14] N = 1.7×10^{22} cm^{-3}, whereas for our samples N = 4.5×10^{22} cm^{-3}. According to the data of[14] the ratio $\nu_{295} : \nu_{90} : \nu_{30} = 1 : 0.8 : 0.5$, while according to the data of this paper $\nu_{293} : \nu_{78} : \nu_{4.2} = 1 : 0.2 : 0.1$ (the subscripts denote the absolute temperature). Both these circumstances are connected with the presence of a distorted surface layer on the mechanically polished samples.

After determining N and ν, we calculated the collision frequencies of electrons with phonons ν_{ep} and with defects ν_{ed}, as well as the values of l and δ in accordance with the formulas[5]

$$\nu = \nu_{ep} + \nu_{ed}, \quad \nu_{ep}^{cl} + \nu_{ed} = 2.533 \cdot 10^8 N/\sigma_{st},$$
$$\frac{\nu_{ed}}{\nu_{ep}^{cl} + \nu_{ed}} = \frac{R_{res}}{R}, \quad l = \frac{\langle v_F \rangle}{\nu}, \quad \delta = \frac{\lambda}{2\pi\varkappa}, \tag{7}$$

Table II. Microcharacteristics of niobium

	$T = 293°$ K	$T = 78°$ K	$T = 4.2°$ K
$N \cdot 10^{-22}$, cm^{-3}	4.49±0.06	4.33±0.14	4.33±0.15
N/N_a	0.82±0.01	0.79±0.03	0.79±0.03
$v_F \cdot 10^{-8}$, cm/sec	0.94±0.01	0.92±0.01	0.92±0.005
$\beta_1/\lambda^2 \cdot 10^4$, μ^{-2}	3.3±0.3	0.63±0.06	0.27±0.03
$\beta_2 \cdot 10^2$	4.8±0.2	22±3	32±4
$\nu \cdot 10^{-14}$, sec^{-1}	2.28±0.04	0.49±0.07	0.29±0.05
$\nu_{ep} \cdot 10^{-14}$, sec^{-1}	2.24±0.17	0.45±0.09	0.25±0.08
$\nu_{ep}^{cl} \cdot 10^{-14}$, sec^{-1}	1.64	0.3	—
$\nu_{ed} \cdot 10^{-14}$, sec^{-1}	0.04	0.04	0.04
$S_F \cdot 10^{37}$, g^{2}cm^2/sec^2	2.26	2.23	2.23
$l \cdot 10^6$, cm	0.41	1.9	3.2
$\delta \cdot 10^6$, cm	3.1	2.6	2.6
V_{110}, eV	1.18±0.05	1.14±0.04	1.14±0.04
V_{200}, eV	1.89 [16]	—	—
$N \cdot 10^{-22}$, cm^{-3} } calculated	4.1	—	—
N/N_a } from V_g	0.75	—	—

where ν_{ep}^{cl} is the classical collision frequency of elec-
trons with phonons, σ_{st} is the static conductivity,
R_{res}/R is the ratio of the residual resistance to the re-
sistance at a temperature T. The measured values of
σ_{st} and R_{res}/R for the investigated samples turned out
to be:

	$T = 293°K$	$T = 78°K$
σ_{st}, cgs esu:	$0.59 \cdot 10^{17}$	$2.91 \cdot 10^{17}$
R_{res}/R:	~ 0.25	~ 0.13

The values of ν_{ep}, ν_{ed}, ν_{ep}^{cl}, l, and δ are given in
Table II.

2. Short-wave region. In the $0.4-5.0\,\mu$ range the
optical properties are determined both by the conduc-
tion electrons and by the electrons participating in
interband transitions. In processing the experimental
data we made use of the additivity of the complex dielec-
tric constant ϵ'. The calculation was carried out in ac-
cordance with the formulas

$$\varepsilon = \varepsilon_e + \tilde{\varepsilon}, \quad \sigma = \sigma_e + \tilde{\sigma},$$

where $\epsilon = \text{Re } \epsilon'$, $-4\pi\sigma/\omega = \text{Im } \epsilon'$; ϵ_e and σ_e refer to the
conduction electrons, and $\tilde{\epsilon}$ and $\tilde{\sigma}$—to interband transi-
tions.

The contribution of the conduction electrons was de-
termined by means of the microcharacteristics obtained
in the long-wave spectral range (see Table II) according
to the formulas[7,8]

$$\varepsilon_e = -\frac{(3,1826 \cdot 10^3 N)^2}{\omega^2 + \nu^2}(1 - B_1), \quad B_1 = \beta_1 + \frac{2\nu^2}{\omega^2 + \nu^2}(\beta_2 - \beta_1),$$

$$\sigma_e = 253.26\frac{N\nu}{\omega^2 + \nu^2}(1 - B_2), \quad B_2 = \beta_2 + \frac{2\omega^2}{\omega^2 + \nu^2}(\beta_1 - \beta_2). \quad (8)$$

The dependence of the interband conductivity $\tilde{\sigma}$ on the
photon energy is shown in Fig. 5. It is seen from Fig. 5
that in the $2-3$ eV region $\tilde{\sigma}$ has the principal maximum
which changes little on going over from helium to nitro-
gen temperature. At room temperature it is somewhat
broader and lower. The positions of the maxima corre-
spond to 2.50, 2.40, and 2.42 eV for temperatures of
293, 78, and 4.2°K. The error in the determination of
the parameters of the conduction electrons has prac-
tically no effect on the positions of the maxima since
their contribution in this region is less than 1 percent.

In addition to the above, there are two other maxima
which appear clearly at nitrogen and helium tempera-
tures. The positions correspond to 0.56 and 0.32 eV.
Only a change of the smooth course of the $\tilde{\sigma}(\hbar\omega)$ curve
is observed in this region at room temperature. Chang-
ing the parameters of the conduction electrons within
the errors with which they have been determined does
not shift the position of the first maximum, whereas the
position of the second maximum shifts by ±0.07 eV. In
addition to the above maxima, there is a deviation of
the smooth course of the $\tilde{\sigma}(\hbar\omega)$ curve in the region of
0.9 eV.

At room temperature the maxima of the light conduc-
tivity were obtained in[16,17]. Two principal maxima of
σ at 4.0 and 2.2 eV were determined in the paper of
Kirillova and Charikov.[16] A comparison with our data
shows that the displacement of the second maximum is
small—on the order of 12 percent, whereas its magni-
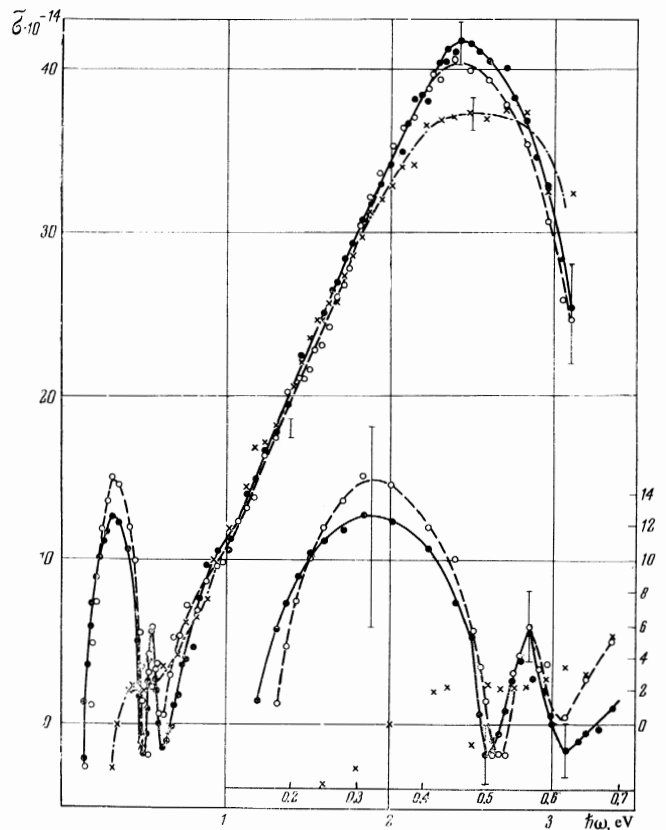tude is smaller by about a factor of one and one half.

FIG. 5. Interband conductivity of niobium: $\times - T = 293°K$, $\bullet -$
$T = 78°K$, $\circ - T = 4.2°K$.

The data of Lenham's work[17] disagree with our data
much more strongly, a fact which again attests to the
strongly deformed surface layer of the samples used
in[17].

The parameters of the band of the interband transi-
tion are presented in Table III which includes ω_{max}—
the frequency corresponding to the maximum of the
given band; $\sigma_{max} = \tilde{\sigma}(\omega_{max})$ and $\gamma = \Delta\omega/\omega_{max}$—the
relative broadening of the energy levels[6] where
$\Delta\omega = \omega_{max} - \omega_1$; $\omega_1 < \omega_{max}$ and ω_1 is obtained from the
condition $\tilde{\sigma}(\omega_1) = 0.7\,\tilde{\sigma}(\omega_{max})$.

Figure 6 shows the dependence of the interband
dielectric constant $\tilde{\epsilon}$ on the photon energy $\hbar\omega$ for helium
and room temperature. The $\tilde{\epsilon}(\hbar\omega)$ curves have a compli-
cated structure which washes out with increasing tem-
perature. It should be noted that the principal $\tilde{\sigma}$ bands
correspond to clearly exhibited regions of anomalous
dispersion of $\tilde{\epsilon}$. For $\hbar\omega \approx 3$ eV, $\tilde{\epsilon}$ becomes negative.

DISCUSSION OF THE OBTAINED RESULTS

A free niobium atom has the valence configuration
$4d^45s^1$; because of strong interaction, the s and d states
in a metal are mixed forming a common Fermi surface.
An attempt is made below to consider the optical proper-
ties of niobium on the basis of the weak-coupling ap-
proximation.

1. The fundamental structure of the bands of the
interband conductivity as well as the optical constants
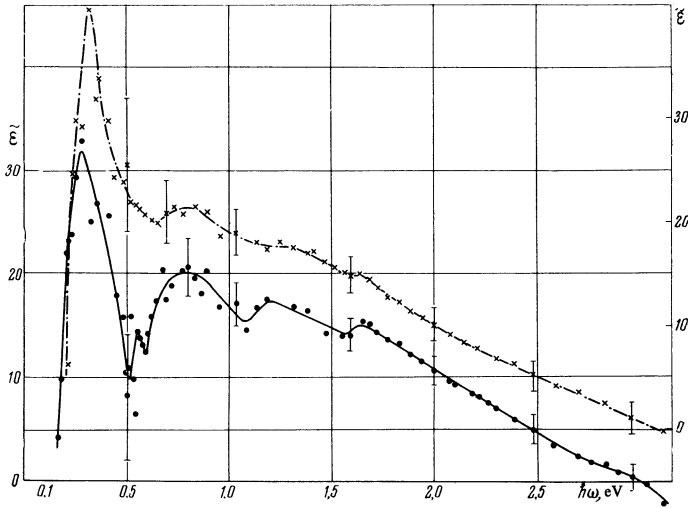in the infrared region depend essentially on the Fourier

FIG. 6. Interband dielectric constant of niobium: X — T = 293°K (right-hand ordinate axis). O — 4.2°K (left-hand ordinate axis),

components of the pseudopotential which correspond to the Bragg planes intersecting the Fermi surface. Let us find these planes. Niobium has a body-centered cubic lattice. For this lattice the dependence of the radius of the free-electron sphere p_F^0 on the valence η is shown in Fig. 7. The horizontal lines mark the distances from the center of the zone to the Bragg planes for which the structure factor does not vanish (the indices of the physically equivalent Bragg planes are shown in curly brackets). It is seen from the Figure that for $\eta = 5$ the Fermi surface will be intersected by the {110} and {200} planes. This leads to the following.

First, two principal bands should be observed on the curve of the frequency dependence of the interband conductivity. The positions of the maxima of these bands are related to the values of the Fourier components of the pseudopotential V_g (g is the subscript of the appropriate Bragg plane) by the relation

$$|V_g| = \hbar\omega_{g\,max} / 2t_g, \tag{9}$$

where $\omega_{g\,max}$ is the frequency corresponding to the maximum of the interband conductivity, and t_g is a coefficient of the order of unity which depends on the relative broadening of the energy levels calculated in[6].

Secondly, the concentration of conduction electrons N should be much less than that of the valence electrons,

N_{val}. It is given by the relations[4,8]

$$\frac{N_{val}-N}{N_{val}} = 6.27\frac{|V_{110}|}{E_F^0}\left(\frac{1}{2}+\frac{\varphi_{110}}{\pi}\right)+4.44\frac{V_{200}}{E_F^0}\left(\frac{1}{2}+\frac{\varphi_{200}}{\pi}\right),$$

$$\varphi_{110} = \text{arctg}\frac{2(p_{110}/p_F^0)[1-(p_{110}/p_F^0)]}{|V_{110}|/E_F^0},$$

$$\varphi_{200} = \text{arctg}\frac{2(p_{200}/p_F^0)[1-(p_{200}/p_F^0)]}{|V_{200}|/E_F^0}. \tag{10}$$

Here $E_F^0 = (p_F^0)^2/2m$, $p_F^0 = 1.06\,(2\pi\hbar/a)$, a is the lattice constant, and m is the free-electron mass. In (10) allowance has been made for the fact that there are twelve {110} and six {200} planes.

2. The results presented in Table III show that niobium has in fact two principal bands of interband conductivity. They can be interpreted as {110} and {200} bands. The first band in the region of 4.0 eV corresponds to the {200} band and the second band with the maximum in the region of 2.5 eV corresponds to the {110} band. The identification of the first band as the {110} band and of the second band as the {200} band contradicts the data on the concentration of the conduction electrons of niobium.

In order to obtain the values of V_g in accordance with (9), one must find the coefficients t. Using data on the band width of the interband conductivity and the results of the calculation in[6], we find $t_{110} = t_{200} = 1.06$. Hence $V_{200} = 1.89$ eV (T = 293°K) and $V_{110} = 1.18$ eV for

FIG. 7

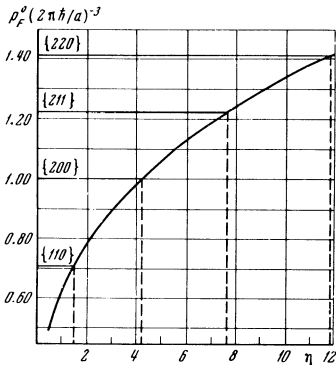**Table III. Band parameters of the interband conductivity of niobium**

No. of band	T, °K	$\hbar\omega_{max}$, eV	$\sigma_{max}\cdot10^{-1}$	$\gamma=\Delta\omega/\omega_{max}$
1*	293	4, 0	—	0. 4
2	293	2.50	37	0.33
	78	2.40	40	0,27
	4.2	2,42	42	0,27
3	78	0.56	6	0.03
	4,2	0.56	6	0,03
4	78	0,32	15	0.3
	4,2	0,32	13	0.3

*According to the results of [16].

T = 293°K, and V_{110} = 1.14 eV for T = 78 and 4.2°K.

3. In addition to the principal bands of the interband conductivity at T = 4.2°K and 78°K, we observed two additional weak maxima. One can assume that they are connected with electron transitions near the lines of intersection of two or the points of intersection of three Bragg planes. The presence of other weaker transitions is also indicated by the complicated structure of the $\bar{\varepsilon}(\hbar\omega)$ curve. However, appropriate calculations of the energy spectrum of niobium are unavailable; this makes it impossible to carry out at present a complete comparison of experiment with theory.

4. The concentration of conduction electrons in niobium is 0.8 electron/atom (see Table II) which is much less than the concentration of valence electrons which is 5 electron/atom. This is evidence of the strong influence of the periodic lattice potential. It should be noted that the concentration of conduction electrons is close to unity, as is also the case for other good metals, independently of their valence.

5. We shall calculate the concentration of conduction electrons N from the obtained values of the Fourier components of the pseudo-potential. For niobium the lattice constant a = 3.30 × 10^{-8} cm (at T = 293°K).[18] This yields E_F^0 = 15.4 eV. From formulas (10) it follows that N = 0.75 electron/atom = 4.1 × 10^{22} electron/cm^3. Experiment gives N = 0.8 electron/atom = 4.5 × 10^{22} electron/cm^3. Thus, the concentration of conduction electrons obtained from measurements in the long-wave region practically coincides with the electron concentration calculated from the Fourier components of the pseudopotential.

6. The measurements indicate that on going from helium to nitrogen temperature N remains practically unchanged, having a value of 4.33 × 10^{22} electron/cm^3. At room temperature it increases to a value of 4.49 × 10^{22} electron/cm^3. The increase of N with increasing temperature is observed in measuring this quantity in the entire 5–10 μ interval. The average value of the ratio N_{293}/N_{78} = 1.03. The sign of the effect for niobium coincides with the sign of the analogous effect for indium, tin, lead, and aluminum, although the temperature dependence of V_{110} is anomalous.[5,7,8,19] This is apparently connected with the fact that the change of N with temperature is basically determined by the temperature variation of V_{200}. Unfortunately nobody has thus far measured the latter dependence.

7. It is seen from Table II that the effective electron collision frequency at T = 293°K is large and amounts to 2.3 × 10^{14} sec^{-1} which is close to the corresponding values for indium and antimony.[6,2,3] However, the temperature dependence of ν in niobium is much larger than in indium and antimony. The main contribution to the values of ν at all temperatures is due to electron-phonon collisions ν_{ep}. The collision frequency of electrons with defects ν_{ed} is 0.04 × 10^{14} sec^{-1} which amounts to ~ 2, 8, and 14 percent of ν for the temperatures 293, 78, and 4.2°K respectively.

Figure 8 shows the experimental data for ν_{ep} at three temperatures, as well as the theoretical ν_{ep}(T) curve taken from[20]. Here Θ is the Debye temperature and ν_Θ = 0.94 $\nu_{ep}(\Theta)$. Experiment shows a stronger decrease of ν_{ep} on decreasing the temperature than pre-
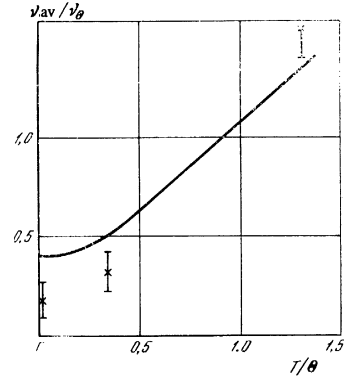

FIG. 8. Dependence of the collision frequency of the electrons with phonons ν_{ep}/ν_Θ: on the temperature T/Θ: points — experiment, curve — theory. [20].

dicted by the Gurzhi-Holstein theory.[20,21] However, this discrepancy is considerably smaller than the discrepancy with the classical theory. Thus, according to experiment ν_{ep}(293°K)/ν_{ep}(4.2°K) ≈ 9; according to the Gurzhi-Holstein theory the ratio is 3.4; according to classical theory it is 7 × 10^5.[22] Thus, for the optical properties of niobium, as well as those of other metals, the essential role is played by the quantum nature of the photon-phonon interaction.

8. Making use of the values of the coefficients γ (Table III) and of the uncertainty relation, one can estimate the effective collision frequency ν_g of electrons taking part in interband transitions in accordance with the formula[8]

$$\nu_g \sim 4\gamma |V_g| / \hbar. \tag{11}$$

This quantity turns out to be of the order of 2 × 10^{15} sec^{-1} which is much larger than the effective collision frequency of the electrons on the Fermi surface ν. In addition, the temperature dependence of ν_g is much smaller than the temperature dependence of ν. Possible reasons for such large values of ν_g are indicated in[6,8].

Thus a discussion of the obtained results shows that both the general structure of the bands of the interband conductivity and the concentration of conduction electrons of niobium agree with the result of the theory based on the weak-coupling approximation.

[1] A. I. Golovashkin, G. P. Motulevich, and A. A. Shubin, Zh. Eksp. Teor. Fiz. 38, 51 (1960) [Sov. Phys.-JETP 11, 38 (1960)].

[2] A. I. Golovashkin and G. P. Motulevich, Zh. Eksp. Teor. Fiz. 47, 64 (1964) [Sov. Phys.-JETP 20, 44 (1965)].

[3] A. I. Golovashkin and G. P. Motulevich, Zh. Eksp. Teor. Fiz. 46, 460 (1964) [Sov. Phys.-JETP 19, 310 (1964)].

[4] R. N. Gurzhi and G. P. Motulevich, Zh. Eksp. Teor. Fiz. 51, 1220 (1966) [Sov. Phys.-JETP 24, 818 (1967)].

[5] A. I. Golovashkin, I. S. Levchenko, G. P. Motulevich, and A. A. Shubin, Zh. Eksp. Teor. Fiz. 51, 1622 (1966) [Sov. Phys.-JETP 24, 1293 (1967)].

[6] A. I. Golovashkin, A. I. Kopeliovich, and G. P. Motulevich, ZhETF Pis. Red. 6, 651 (1967); Zh. Eksp. Teor. Fiz. 53, 2053 (1967) [JETP Lett. 6, 142 (1967); Sov. Phys.-JETP 26, 1161 (1968)].

[7] A. I. Golovashkin and G. P. Motulevich, Zh. Eksp. Teor. Fiz. 53, 1526 (1967) [Sov. Phys.-JETP 26, 881 (1968)].

[8] G. P. Motulevich, Dissertation, Moscow, FIAN, 1968.

[9] G. P. Motulevich and A. A. Shubin, Optika i spektroskopiya 2, 633 (1957).

[10] P. A. Jaquet, Le polissage electrolytique des surfaces metalliques et ses applications. St. Germain-en-Laye, 1948.

[11] I. E. Leksina, G. P. Motulevich, L. N. Fedotov, and A. A. Shubin, FMM 23, 511 (1967).

[12] M. M. Kirillova and B. A. Charikov, FMM 16, 205 (1963).

[13] A. P. Lenham and D. M. Treherne, J. Opt. Soc. Am. 56, 1137 (1966).

[14] A. P. Lenham and D. M. Treherne, J. Opt. Soc. Am. 57, 476 (1967).

[15] G. P. Motulevich, Zh. Eksp. Teor. Fiz. 46, 287 (1964) [Sov. Phys.-JETP 19, 199 (1964)].

[16] M. M. Kirillova and B. A. Charikov, FMM 19, 495 (1965).

[17] A. P. Lenham, J. Opt. Soc. Am. 57, 473 (1967).

[18] W. Pearson, A Handbook of Lattice Spacings and Structures of Metals and Alloys, Pergamon, 1958.

[19] G. P. Motulevich, Eksp. Teor. Fiz. 51, 1918 (1966) [Sov. Phys.-JETP 24, 1287 (1967)].

[20] R. N. Gurzhi, Zh. Eksp. Teor. Fiz. 33, 451, 660 (1957) [Sov. Phys.-JETP 6, 352, 506 (1958)]; Dissertation, Khar'kov, FTI AN USSR, 1958.

[21] T. Holstein, Phys. Rev. 96, 535 (1954).

[22] Low-temperature Physics, Handb. Physik v. 14—15, Springer, 1956.